The benchmark of LiDAR odometry algorithms utilised for a low-cost mobile mapping system

Janusz Będkowski [1,2], Marcin Matecki [1,3], Michał Pełka [4], Karol Majek [5], Przemysław Lekston [5], Adam Kostrzewa [6,7], Jakub Markiewicz [6], Sławomir Łapiński [6], Michał Własiuk [2], Kornel Mrozowski [2]

[1] Institute of Fundamental Technological Research, Polish Academy of Sciences, Poland - januszbedkowski@gmail.com
[2] Samsung Electronics
[3] IDEAS Research Institute, Warsaw, Poland - matecki.m@outlook.com
[4] Robotec sp. z o.o., Koszykowa 61b, 00-661 Warsaw – michalpelka@gmail.com
[5] Citizen Scientist - (karolmajek, p.lekston)@gmail.com
[6] Warsaw University of Technology, Faculty of Geodesy and Cartography, Plac Politechniki 1, 00-661 Warsaw, Poland - (adam.kostrzewa.dokt, jakub.markiewicz, slawiomir.lapinski)@pw.edu.pl
[7] Institute of Civil Engineering, Warsaw University of Life Sciences, Nowoursynowska 166, 02-787 Warsaw, Poland - adam_kostrzewa@sggw.edu.pl

Keywords: low-cost, open-source software, LiVOX MID360, point cloud registration algorithms, mobile mapping, benchmark

Abstract

In recent years, the development of Mobile Mapping Systems (MMS) has seen a noticeable increase, particularly those based on low-cost sensors for acquiring various geospatial data. This has contributed to the growth in the number of different applications, and mobile mapping is now widely used, for example, in autonomous vehicles, photogrammetric Unmanned Aerial Vehicle (UAV) missions, and various navigation applications and the MMS is also considered a method of mobile space inventory. Another significant application of MMS is the continuous development of building interior mapping technology to analyse the construction process and create applications that support the movement of people, especially for emergency services or people with disabilities. A benchmark of current SOTA LiDAR odometry algorithms was proposed. It is available at MapsHD/HDMapping. A benchmark of 20 algorithms: CT-ICP, DLIO, DLO, FASTER-LIO, FAST-LIO, GenZ-ICP, GLIM, i2ekf-lo, ig-lio, KISS-ICP, LeGO-LOAM, LiDAR_IMU_Init, LIO-EKF, LIO-SAM, LOAM, MAD-ICP, POINT-LIO, RESPLE, SLICT and VOXELMAP was conducted in the laboratory and challenging Bunker DVI Dataset.

1. Introduction

In recent years, the development of Mobile Mapping Systems (MMS) has seen a noticeable increase, particularly those based on low-cost sensors for acquiring various geospatial data. This has contributed to the growth in the number of different applications, and mobile mapping is now widely used, for example, in autonomous vehicles, photogrammetric unmanned aerial vehicle missions, and various navigation applications and the MMS is also considered a method of mobile space inventory. Another significant application of MMS is the continuous development of building interior mapping technology to analyse the construction process and create applications that support the movement of people, especially for emergency services or people with disabilities.

The crucial aspect related to the use of MMS is the workflow of data acquisition and processing, which consists of the following steps: (1) evaluation of data collected from individual sensors, (2) data registration aimed at creating a consistent dataset, (3) data filtering, and (4) generation of final documentation based on the processed data, depending on project's objectives. For this reason, it is necessary to research emerging system prototypes, evaluate the quality of new applications and sensors, compare solutions and algorithms utilised for data processing, and search for new, optimal systems.

Open source solutions have become very popular due to the open nature of these tools, which allows for broad collaboration within the research community and rapid innovation (Kostrzewa et al., 2025). In addition, their transparency and lack of licensing costs encourage widespread use in scientific research and commercial applications.

Low-cost solutions have also become popular. The low cost of entry allows smaller research institutions, startups, and local governments that do not have large budgets to test and implement the technology. In addition, such systems often prove sufficient for many inventory tasks and experimental applications where the highest measurement accuracy is not required.

LiDAR odometry is a fundamental technique in robotic navigation that estimates the motion of a platform by analysing sequential 3D point clouds captured by LiDAR sensors. Unlike visual odometry, LiDAR-based methods are highly robust in environments with poor lighting or texture, making them suitable for autonomous vehicles, drones, and mobile robots operating in diverse conditions. The core principle involves registering consecutive LiDAR scans to compute relative transformations, often using methods such as Iterative Closest Point (ICP), feature extraction, and probabilistic optimisation. Many modern algorithms also incorporate inertial data from IMUs to enhance robustness and accuracy, especially in dynamic or geometrically degenerate environments.

Recent surveys highlight the diversity and evolution of LiDAR odometry approaches. For example, Liu et al. (2025) provide a comprehensive review of LiDAR odometry and mapping innovations, emphasising the integration of probabilistic models and sensor fusion techniques. Similarly, Lee et al. (2024) discuss the challenges of generalisation and real-time performance across different platforms and environments. Potokar and Kaess (2025) offer a detailed evaluation of state-of-the-art algorithms, comparing their performance on benchmark datasets such as KITTI and MulRan (Potokar and Kaess, 2025). Despite significant progress, challenges remain in achieving scalable,

real-time, and loop-closure-capable odometry systems. Ongoing research continues to refine these methods, aiming for more generalisable and efficient solutions.

This article evaluates the quality of LiDAR odometry algorithms CT-ICP (Dellenbach et al., 2022), DLO (Chen et al., 2022), FASTER-LIO (Bai et al., 2022), FAST-LIO (Xu and Zhang, 2021), GenZ-ICP (Lee et al., 2025), GLIM (Koide et al., 2024), i2ekf-lo (Yu et al., 2024), ig-lio (Chen et al., 2024), KISS-ICP (Vizzo et al., 2023), LeGO-LOAM (Shan and Englot, 2018), LiDAR_IMU_Init (Zhu et al., 2022), LOAM (Zhang et al., 2014), SLICT (Nguyen et al., 2023), VOXELMAP (Yuan et al., 2022) used for registering low-cost point clouds from the MMS Mandeye mobile mapping system equipped with a LIVOX MID360 LiDAR. Table 1 presents the description of each method's advantages and disadvantages. The research was conducted in the CENAGIS laboratory of the Warsaw University of Technology (WUT). The point cloud from the MMS was compared with a reference Terrestrial Laser Scanning (TLS) point cloud from Leica RTC 360.

This benchmark compares several groups of LiDAR odometry algorithms, including:
- Iterative Closest Point (CT-ICP, GenZ-ICP, KISS-ICP);
- Feature based 3D-LiDAR odometry (LOAM, LeGO-LOAM);
- Graph optimisation based 3D LiDAR SLAM (LeGO-LOAM, SLICT);
- Filter-based 3D LiDAR SLAM (FAST-LIO, FAST-LIO2 and FASTER-LIO, I2EKF-LO, Point-LIO, VoxelMap).

Additionally, these algorithms can be separated into LiDAR Odometry only and LiDAR-Inertial Odometry (LIO) algorithms. LO-only odometry includes CT-ICP, DLO, GenZ-ICP, I2EKF-LO, and KISS-ICP. All remaining algorithms support the LIO approach, where some, like LeGO-LOAM, indicate that the use of IMU is optional. LIO algorithms combine precise LiDAR point clouds with IMU data for enhanced state estimation. This approach typically excels in highly dynamic use cases. Notable implementations include LIO-SAM (Shan et al., 2020) using factor graphs and Fast-LIO (Xu and Zhang, 2021), achieving real-time performance through efficient point cloud registration.

2. Related works

MMS must operate within several hard constraints, like the compute capacity of the mobile platform, real-time, low-power requirements, and characteristics of the main sensing device. What's more, these systems are expected to deliver high accuracy measurements in varying environments and remain robust in the presence of dynamic motion.

The evaluated algorithms implement varying methods to address these constraints. LeGO-LOAM (Shan and Englot, 2018) relies on feature extraction from point cloud to obtain distinctive planar and edge features. It is reported to achieve real-time pose estimation on a low-power embedded system. However, its design is optimised strictly for horizontally placed LiDARs installed on ground vehicles. The inherent assumption of this algorithm is that the ground plane is always observed in each scan, and it is further leveraged in its segmentation and optimisation steps.

In the KISS-ICP (Vizzo et al., 2023) paper, the authors propose a minimalistic approach to LiDAR odometry that aims to simplify their system's overall complexity. Authors identify point-to-point ICP with a robust kernel (Chebrolu et al., 2021), adaptive correspondence matching, motion compensation and a point subsampling strategy as the minimal set of components that can be successfully employed to provide stable results on a wide range of sensors and in varying environments. KISS-ICP intentionally moves back from the increasing popularity of pose-graph approaches and proposes a system that solely relies on a point-to-point metric.

Authors of GenZ-ICP (Lee et al., 2025) focused on the fact that the accuracy of LiDAR odometry varies depending on the environment and often deteriorates in long corridors, tunnels or similar degenerative environments. This issue is attributed to the dependence on a single error metric, which has different strengths and weaknesses depending on the geometrical characteristics of the surroundings. GenZ-ICP authors propose a complementary use of both point-to-plane and point-to-point error metrics, along with adaptive weights to address such degenerative environments.

The Continuous-Time ICP (Dellenbach et al., 2022) paper proposes a real-time LiDAR odometry that aims to tackle highly dynamic motion of the main sensor by introducing combined continuity in the scan matching and discontinuity between scans. The former allows handling the elastic distortion of the scan during the registration for increased precision, and the latter increases robustness to high-frequency motions from the discontinuity. Authors demonstrate the robustness and speed of this approach on multiple published datasets.

VoxelMap (Yuan et al., 2022) proposes a mapping method with plane merging that aims to improve the accuracy and efficiency of LO and LIO algorithms. In this approach, the map is a collection of voxels (each containing one plane feature) organised by a Hash table and octrees to build and update the map efficiently. The proposed voxel map is then fed to an iterated extended Kalman filter to construct a maximum a posteriori probability problem for pose estimation.

FastLIO (Xu and Zhang, 2021) fuses LiDAR feature points with IMU data using a tightly-coupled iterated extended Kalman filter. Authors apply a new formula to calculate Kalman gain to reduce the computational complexity, thus allowing a real-time operation of their algorithm at 40Hz on board a flying quadrotor.

FastLIO2 moves back from extracted features (used to reduce map size) to rely on raw points to improve overall accuracy and offer wider support for distinct scanning patterns of various LiDARs. An incremental K-D tree is introduced to compensate for the increased map and maintain real-time performance.

FasterLIO (Bai et al., 2022) builds on top of that by replacing the K-D tree from FastLIO2 with a sparse, incremental voxel-based representation of the map. Authors argue that the strict k-NN searches (the main benefit of K-D trees) are typically not needed, as in LIO systems, pre-integration can offer a good initial guess of where to search. Hence, FasterLIO is able to find matching correspondences while relying on a limited depth of search by using a voxel based representation.

No.	Algorithm	Working Principle	Advantages	Disadvantages	Reference
1	CT-ICP	Continuous-time ICP with elastic scan matching and loop closure detection	Very accurate (KITTI RTE 0.59%), robust to fast motion, real-time capable	High computational demands at full precision	(Dellenbach et al., 2022)
2	DLIO	DLIO fuses LiDAR and IMU data in a tightly-coupled, continuous-time framework, constructs trajectories using a coarse-to-fine approach, and performs fast, point-wise deskewing with a nonlinear observer for precise motion correction.	architecture is nearly 20% more computationally efficient than DLO, CT-ICP, LIO-SAM, and FAST-LIO2, with a ~12% increase in trajectory accuracy.	LiDAR and IMU sensors need to be properly time-synchronized, otherwise DLIO will not work	(Chen et al., 2022)
3	DLO	Direct registration of dense point clouds with efficient keyframing and NanoGICP	Lightweight, fast, suitable for limited resources, robust in challenging conditions	No deskewing, no IMU integration, limited robustness in dynamic scenes	(Chen et al., 2022)
4	FASTER-LIO	Tightly-coupled LIO with parallel voxel-based processing (iVox)	Extremely fast (up to 2000 Hz), lightweight, supports various LiDAR types	Sensitive to voxel parameters, requires careful tuning	(Bai et al., 2022)
5	FAST-LIO	Tightly-coupled iterated Kalman Filter with deskewing and improved Kalman gain	High accuracy, UAV-compatible, robust to degeneracy	High computational complexity, requires IMU and good calibration	(Xu and Zhang, 2021)
6	GenZ-ICP	ICP with adaptive weighting between point-to-plane and point-to-point based on scene geometry	Robust to degeneracy (e.g., corridors), adaptable to various environments	More complex than classic ICP, it requires planarity analysis	(Lee et al., 2025)
7	GLIM	GPU-accelerated SLAM with fixed-lag smoothing and global scan matching optimisation	Highly accurate, robust to degeneracy, supports multi-sensor fusion	Requires a powerful GPU and a complex implementation	(Koide et al., 2024)
8	I2EKF-LO	Dual-iteration EKF with dynamic noise estimation and distortion compensation	High accuracy, efficient, robust to complex motion	Requires good initialisation, complex to implement	(Yu et al., 2024)
9	iG-LIO	Incremental GICP + IMU in a MAP framework with voxel-based surface estimation	Efficient, supports various LiDAR types, good mapping quality	May struggle in very open or narrow scenes	(Chen et al., 2024)
10	KISS-ICP	Simple point-to-point ICP with adaptive thresholding and subsampling	Very simple, fast, IMU-free, universal	No deskewing, limited robustness to fast motion	(Vizzo et al., 2023)
11	LeGO-LOAM	Ground segmentation + feature extraction + two-stage Levenberg-Marquardt optimisation	Lightweight, optimised for ground vehicles, embedded-friendly	Not optimal for UAVs, depends on ground plane presence	(Shan and Englot, 2018)
12	LiDAR_IMU_Init	Calibration of temporal and spatial offsets between LiDAR and IMU using Ceres Solver	Real-time, no special conditions needed, supports various LiDARs	Requires sufficient motion excitation, limited IMU support in the basic version	(Zhu et al., 2022)
13	LIO-EKF	A tightly coupled LiDAR–inertial odometry using point-to-point scan registration within a classical Extended Kalman Filter framework.	Provides accurate, high-frequency (≈100 Hz) LiDAR–inertial odometry using a simple EKF framework, achieving state-of-the-art performance near IMU rate.	Issue with running with our datasets	(Wu et al., 2023)
14	LIO-SAM	Tightly-coupled LiDAR–inertial odometry using factor graph optimization with local scan-matching, IMU pre-integration, and loop closure incorporation.	Provides real-time, tightly coupled LiDAR–inertial odometry with multi-sensor fusion and local scan-matching, achieving accuracy comparable to or exceeding LOAM and LIOM.	Issue with running with our datasets	(Shan et al., 2020)
15	LOAM	Splits task into fast odometry and slower mapping; uses edge and planar features	Low computational cost, good accuracy, IMU-free	No loop closure, prone to drift over long trajectories	(Zhang et al., 2014)
16	MAD-ICP	MAD-ICP is a LiDAR odometry system based on the ICP paradigm, using a PCA-based kd-tree	Provides robust, adaptive LiDAR odometry with local map updates to limit drift, efficient computation reuse, real-time open-source implementation, and validated accuracy across diverse datasets (KITTI, Mulran, Newer College).	Issue with running with our datasets	(Ferarri et al., 2024)
17	POINT-LIO	Point-LIO is a loosely-coupled LiDAR–inertial odometry system that updates the state point-by-point for each LiDAR measurement and uses a stochastic process-augmented kinematic model treating IMU data as outputs, enabling high-frequency, robust odometry during aggressive motions.	Provides high-frequency (4–8 kHz), robust LiDAR–inertial odometry with eliminated in-frame distortion, accurate tracking under aggressive motions, multi-platform support, and performance comparable to state-of-the-art LIO systems(FAST-LIO2, LILI-OM, LIO-SAM, and LINS)	Issue with running with our datasets	(He et al., 2023)

18	RESPLE	Continuous-time 6-DoF motion estimation using B-splines with an iterated Extended Kalman Filter for recursive Bayesian estimation, enabling real-time odometry with one or multiple LiDARs and an IMU	Provides continuous-time 6-DoF motion estimation with B-splines, efficient EKF-based state estimation, multi-LiDAR/IMU support, real-time performance, and accuracy comparable to T-LO, C-MLO, and F-LIO2.	Issue with running with our datasets	(Cao et al., 2025)
19	SLICT	Surfel-based continuous-time odometry with multi-scale association and B-spline optimisation	High accuracy, robust to degeneracy, real-time capable	High implementation complexity, requires ROS Noetic and Ceres Solver	(Nguyen et al., 2023)
20	VOXELMAP	Adaptive voxel mapping with planar representation and uncertainty modelling; uses MAP and IEKF	Efficient, probabilistic, performs well in challenging environments	High memory usage with full uncertainty modelling, limited IMU support in the basic version	(Yuan et al., 2022)

Table 1. The description of the utilised LIDAR odometry algorithms

SLICT (Nguyen et al., 2023) offers another approach to efficiently use voxel maps by proposing an octree-based global map. The advantage of this approach is that the index of the global map can be updated incrementally. Authors propose a novel point-to-surfel association and integrate with IMU preintegration factors in a joint pose-graph.

IG-LIO (Chen et al., 2024) presents a tightly coupled LiDAR-IMU odometry, which proposes a Generalised ICP approach. It uses a voxel-based surface covariance estimator and an incremental voxel map to reduce the time consumption of overall computations.

Finally, various other implementations of LiDAR-based SLAM systems are also investigated in Yue et al. (Yue et al., 2023), who provide a comprehensive survey of LiDAR-based SLAM algorithms and their main building blocks. The authors inspect LIDAR-based SLAM systems according to the growing complexity of their components and discuss several applications of such systems.

The description of the algorithms used in this work is presented in Table 1. The main advantages and disadvantages of the solutions and the principle of operation are also presented.

The contribution of this paper is as follows:

- Novel extensive LiDAR odometry algorithms benchmark incorporating different laboratory conditions (acceleration, speed) and available SOTA benchmark data
- New dataset with ground truth (varying different acceleration, speed)
- Qualitative and quantitative evaluation of SOTA LiDAR odometry algorithms in laboratory and realistic conditions

3. Material and methods

3.1 Laboratory Setup

The experiments were conducted at the WUT - CENAGIS (Centre for Spatial and Satellite Analyses), which enables the testing and validation of active and passive measurement sensors. It is a unique research infrastructure located in the main building of the scientific and educational centre and the Astronomical and Geodetic Observatory of the Warsaw University of Technology. The laboratory integrates several specialised components: advanced IT infrastructure for geospatial analysis and satellite data processing (including large spatial data sets) and calibration and certification laboratories for measuring devices to acquire geoinformation. This enables the testing, calibration, and accuracy assessment of various geodetic sensors (including cameras, laser scanning systems, rangefinders, and GNSS receivers), positioning systems (external and internal), and navigation applications.

One of the key components of the laboratory experiment is the Bosch-Rexroth linear measuring rail with a trolley (Table 2), which allows linear and non-linear movements at acceleration up to 15 m/s^2. This tool allows for the controlled movement of test objects in laboratory conditions and is widely used in research (Markiewicz et al., 2022):

- evaluating the accuracy of measuring systems and devices in motion,
- analysing distance and angular accuracy,
- testing SLAM algorithms,
- studying the impact of the Rolling Shutter phenomenon on measurement results.

A straight guide with a trolley enables controlled movement of test objects, allowing for testing the accuracy of measurement systems in motion. It is advantageous in assessing the accuracy of distance determination, which is a fundamental element of many measurement techniques, such as TLS and tachymetric measurements, while referencing the SI unit of length – the meter. In the experiment, the rail was used to impart a controlled speed to the MMS system and to change speed and acceleration. This allowed for the robustness of point cloud registration algorithms to be analysed concerning different motion conditions and measurement dynamics.

Length	9.3 m
Max. speed of the trolley	5 m/s
Max. acceleration of the trolley	10 m/s^2
Max. weight of the devices/MMS	25 kg
The vibration-damping function	The actuator is equipped with a frequency-dependent vibration-damping function.
Trolley	The mobile trolley, including a table (table dimensions – 250 x 250 mm)
Software Development Kit	The ability to create your own control and monitoring applications
Programming languages	PLCopen, Python, C/C++ and more

Table 2. Main characteristics of the Linear guide

The second key element used in the experiment was a reconfigurable calibration field. It allows for arranging markers and measurement points in 80 designated locations on walls, pillars, and columns, complementing the placement of fixed reference points. Using precise measuring prisms, black-and-white checkerboards, and reference spheres with a diameter of 150 mm makes it possible to flexibly adapt the field to various research scenarios. This approach significantly expands the functionality of the laboratory and allows it to meet the requirements of even the most advanced users (Medić et al., 2019). When combined, the two elements, the reconfigurable calibration field and the rail system, create a unique research environment that enables comprehensive evaluation of the performance of modern mobile mapping systems. Figure 1 presents a general view of the laboratory, including the linear guide system used during the experiments.

Figure 1. General view of the laboratory, including the linear guide system used during the experiments

3.2 Ground truth data

The reference data was obtained using a Leica RTC360 terrestrial laser scanner. The scanning was performed in medium resolution mode, corresponding to an approximate density of 6 mm/10 m and an angular resolution of 0.009° horizontally and 0.009° vertically. Thanks to the built-in HDR imaging camera system, a colour (RGB) point cloud was obtained. The API Radian Pro LaserTracker measurement determined the position of the check points. Table 3 presents error statistics describing the accuracy of check point measurements with respect to the reference data from TLS.

	Total [m]	X [m]	Y [m]	Z [m]
STD	0.002	0.002	0.003	0.001
MIN	0.001	-0.003	-0.021	-0.004
MAX	0.021	0.008	0.008	0.004
Mediana	0.003	0.000	-0.001	0.000
MAD	0.001	0.002	0.002	0.001
SMAD	0.001	0.003	0.003	0.001
RMSE	0.003	0.003	0.003	0.001

Table 3. Error statistics describing the accuracy of check point measurements with respect to the reference data from TLS

A total of 6 scanning stations were performed, which were registered in the Leica Register 360 software. The relative orientation accuracy of the scans was 0.2 cm, while the measurement accuracy on the check points was 0.3 cm.

3.3 Bunker DVI dataset

For evaluation in a realistic and at the same time challenging scenario, the Bunker DVI Dataset (Hamesse et al., 2024) was used, featuring data from LiDAR recorded in challenging conditions reflecting search-and-rescue operations. Below, Figure 2 shows Bunker DVI Dataset.

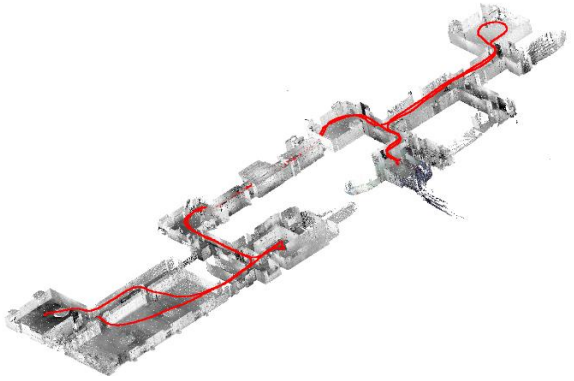

Figure 2. Bunker DVI Dataset (Hamesse et al., 2024), featuring data from LiDAR recorded in challenging conditions reflecting search-and-rescue operations.

A benchmark of CT-ICP, DLIO, DLO, FAST-LIO, FASTER-LIO, GenZ-ICP, GLIM, I2EKF-LO, KISS-ICP, LeGO-LOAM, POINT-LIO, and RESPLE was carried out on data from the Bunker DVI dataset.

3.4 Quantitative evaluation

For quantitative evaluation, ATE (Absolute Trajectory Error, Eq. 1) was used for the position component of the trajectory's poses (Zhang and Scaramuzza, 2018). This error informs the difference between the ground truth trajectory. Ground Truth trajectory was obtained based on mobile LiDAR data registration to the TLS survey:

$$ATE_{pos} = \left(\frac{1}{N} \sum_{i=0}^{N-1} \|\Delta p_i\|^2 \right)^{\frac{1}{2}} \quad (1)$$

where ATE_{pos} = Absolute Trajectory Error
N = number of poses
i = index of pose
Δp = relative position

4. Benchmark

4.1 Laboratory Setup

A mobile mapping system was set up, consisting of two LIVOX MID360 LiDAR sensors mounted orthogonally on a moving track (Figure 3). Twelve consecutive trials were conducted at varying speeds. Figure 4 presents the different speeds, ranging from 4 m/s to 12 m/s, while Figure 5 illustrates the X, Y, and Z displacements of the mobile mapping system during the laboratory trial.

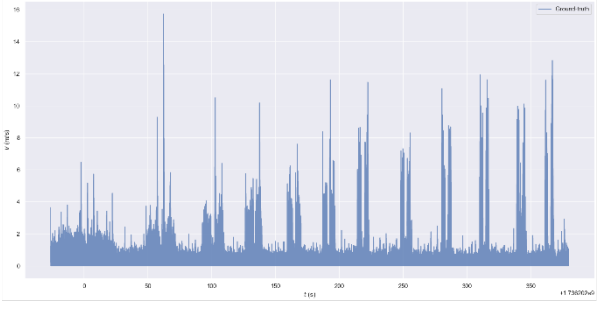

Figure 3. Different speeds from 4m/s up to 12m/s.

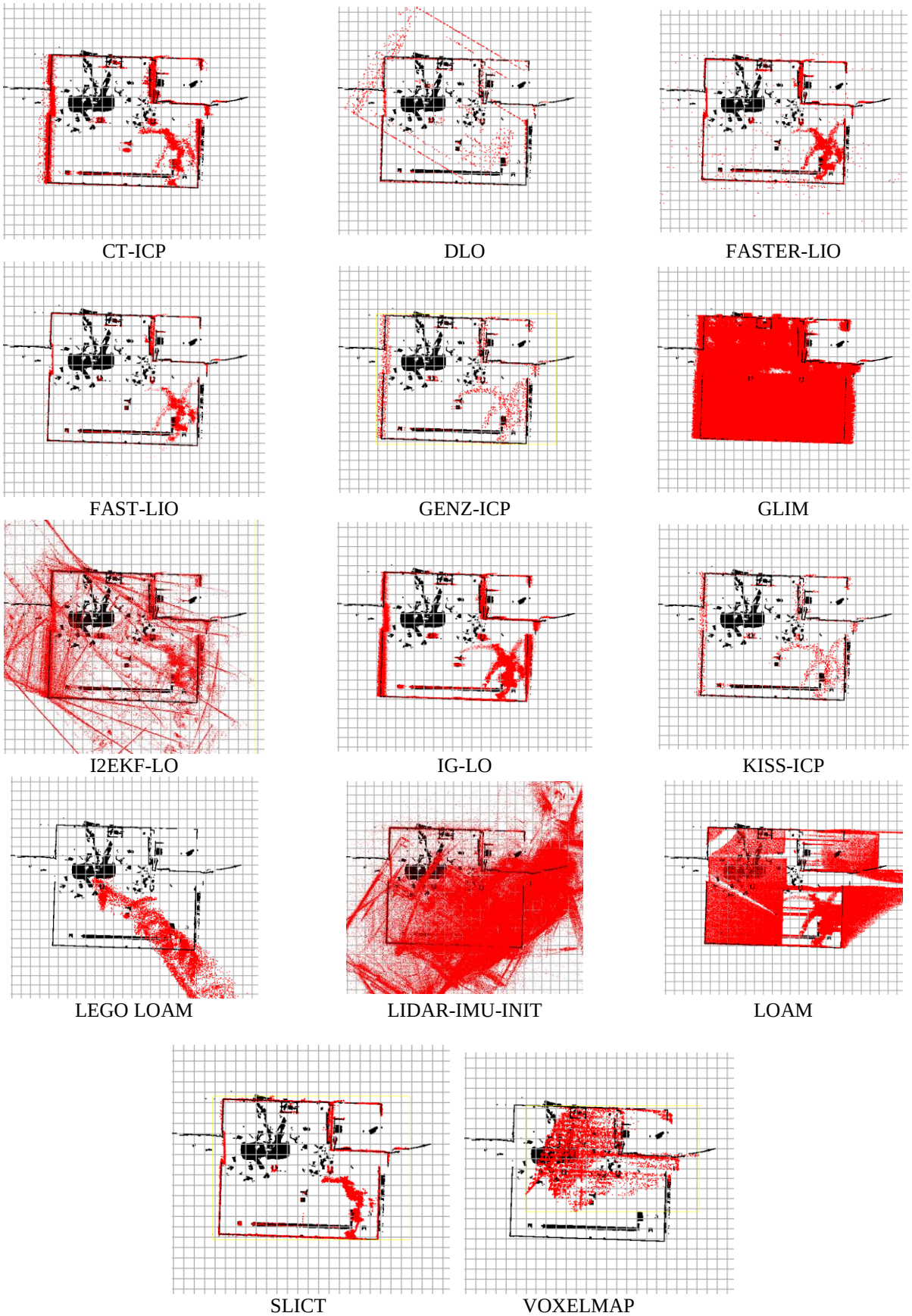

Figure 5. The result of MMS point cloud registration with different algorithms based on laboratory point clouds. Black – ground truth.

https://doi.org/10.5194/isprs-archives-XLVIII-1-W6-2025-25-2025

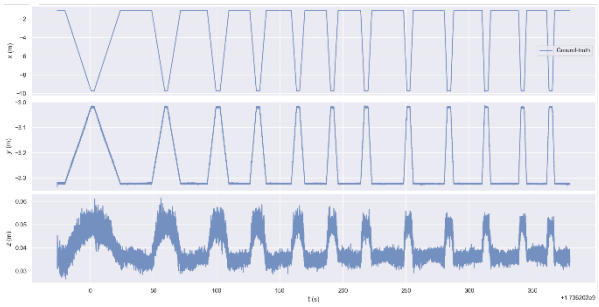

Figure 4. X Y Z displacements of the mobile mapping system during trial.

4.2 Laboratory results

Figure 6 shows the results. Algorithms DLIO, LIO-EKF, LIO-SAM, MAD-ICP, POINT-LIO, and RESPLE failed in these experiments. It can be seen that FASTER-LIO, FAST-LIO and SLICT perform best.

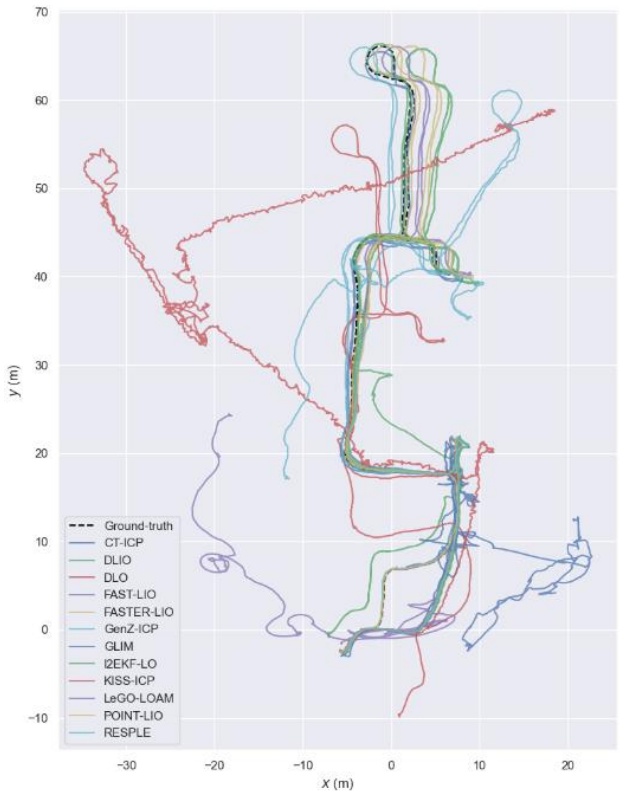

Figure 6. Trajectory comparison in the Bunker DVI dataset

4.3 Quantitative evaluation

For quantitative evaluation, ATE was used for the position component of the trajectory's poses. Table 4 presents the ATE for each trajectory. FASTER-LIO achieved the best performance. Several algorithms (GLIM, KISS-ICP, LeGO-LOAM) failed in this particular experiment.

Algorithm	ATE (Absolute Trajectory Error) [m]
CT-ICP	0.808
DLIO	2.427
DLO	6.242
FASTER-LIO	**0.363**
FAST-LIO	0.890
GenZ-ICP	1.053
GLIM	35.905
I2EKF-LO	0.411
KISS-ICP	23.481
LeGO-LOAM	35.380
POINT-LIO	1.201
RESPLE	9.096

Table 4. Absolute Trajectory Error for LO algorithms evaluated using the Bunker DVI Dataset (Hamesse et al., 2024)

5. Conclusions

A total of 20 algorithms: CT-ICP, DLIO, DLO, FASTER-LIO, FAST-LIO, GenZ-ICP, GLIM, I2EKF-LO, IG-LIO, KISS-ICP, LeGO-LOAM, LiDAR_IMU_Init, LIO-EKF, LIO-SAM, LOAM, MAD-ICP, POINT-LIO, RESPLE, SLICT, and VOXELMAP were benchmarked in both laboratory conditions and using the challenging Bunker DVI Dataset. No results could be obtained in the laboratory setting for DLIO, LIO-EKF, LIO-SAM, MAD-ICP, POINT-LIO, and RESPLE. FASTER-LIO, FAST-LIO, and SLICT achieved the best performance in the laboratory. A benchmark was also conducted for CT-ICP, DLIO, DLO, FASTER-LIO, FAST-LIO, GenZ-ICP, GLIM, I2EKF-LO, KISS-ICP, LeGO-LOAM, POINT-LIO, and RESPLE using the Bunker dataset, revealing significant differences in the resulting trajectories. In this scenario, FASTER-LIO demonstrated the best ATE.

References

Bai, C., Xiao, T., Chen, Y., Wang, H., Zhang, F., Gao, X., 2022: Faster-LIO: Lightweight Tightly Coupled Lidar-Inertial Odometry Using Parallel Sparse Incremental Voxels. *IEEE Robot. Autom. Lett.*, 7, 4861–4868. https://doi.org/10.1109/LRA.2022.3152830

Cao, Z., Talbot, W., & Li, K., 2025: RESPLE: Recursive Spline Estimation for LiDAR-Based Odometry. *IEEE Robot. Autom. Lett.*, 10, 10666 - 10673. https://doi.org/10.1109/LRA.2025.3604758

Chebrolu, N., Läbe, T., Vysotska, O., Behley, J., & Stachniss, C., 2021: Adaptive robust kernels for non-linear least squares problems. *IEEE Robot. Autom. Lett.*, *6*(2), 2240-2247. https://doi.org/10.1109/LRA.2021.3061331

Chen, K., Lopez, B.T., Agha-mohammadi, A., Mehta, A., 2022: Direct LiDAR Odometry: Fast Localization With Dense Point Clouds. *IEEE Robot. Autom. Lett.*, 7, 2000–2007. https://doi.org/10.1109/LRA.2022.3142739

Chen, Z., Xu, Y., Yuan, S., Xie, L., 2024: iG-LIO: An Incremental GICP-Based Tightly-Coupled LiDAR-Inertial Odometry. *IEEE Robot. Autom. Lett.*, 9, 1883–1890. https://doi.org/10.1109/LRA.2024.3349915

Dellenbach, P., Deschaud, J. E., Jacquet, B., & Goulette, F., 2022: Ct-icp: Real-time elastic lidar odometry with loop closure. In *2022 International Conference on Robotics and Automation (ICRA)* (pp. 5580-5586). IEEE.

Ferrari, S., Di Giammarino, L., Brizi, L., & Grisetti, G., 2024: MAD-ICP: It is all about matching data–robust and informed LiDAR odometry. *IEEE Robot. Autom. Lett.*, 9(11). 9175 - 9182. https://doi.org/10.1109/LRA.2024.3456509

Hamesse, C., Vlaminck, M., Luong, H., Haelterman, R., 2024: Depth-Visual-Inertial (DVI) Mapping System for Robust Indoor 3D Reconstruction. *IEEE Robot. Autom. Lett*. 9, 11313–11320. https://doi.org/10.1109/LRA.2024.3487496

He, D., Xu, W., Chen, N., Kong, F., Yuan, C., & Zhang, F., 2023: Point-LIO: robust high-bandwidth light detection and ranging inertial odometry. *Advanced Intelligent Systems*, 5(7), 2200459.

Koide, K., Yokozuka, M., Oishi, S., Banno, A., 2024: GLIM: 3D range-inertial localisation and mapping with GPU-accelerated scan matching factors. *Rob. Auton. Syst.* 179, 104750. https://doi.org/10.1016/j.robot.2024.104750

Kostrzewa, A., Płatek-Żak, A., Banat, P., Wilk, Ł., 2025: Open-Source vs. Commercial Photogrammetry: Comparing Accuracy and Efficiency of OpenDroneMap and Agisoft Metashape. *Int. Arch. Photogramm. Remote Sens. Spat. Inf. Sci*. XLVIII-1/W, 65–72. https://doi.org/10.5194/isprs-archives-XLVIII-1-W4-2025-65-2025

Lee, D., Jung, M., Yang, W., Kim, A., 2024: LiDAR odometry survey: recent advancements and remaining challenges. *Intell. Serv. Robot*. 17, 95–118. https://doi.org/10.1007/s11370-024-00515-8

Lee, D., Lim, H., Han, S., 2025: GenZ-ICP: Generalizable and Degeneracy-Robust LiDAR Odometry Using an Adaptive Weighting. *IEEE Robot. Autom. Lett*. 10, 152–159. https://doi.org/10.1109/LRA.2024.3498779

Liu, G., Huang, K., Lv, X., Sun, Y., Li, H., Lei, X., Yuan, Q., Shu, L., 2025: Innovations and Refinements in LiDAR Odometry and Mapping: A Comprehensive Review. *IEEE/CAA J. Autom*. Sin. 12, 1072–1094. https://doi.org/10.1109/JAS.2025.125198

Markiewicz, J., Gotlib, D., Gnat, M., & Łapiński, S. (2022). One-Stop-Lab CENAGIS: from calibration of surveying devices and application testing to large-scale geodata computation. *FIG Peer Review Journal*.

Medić, T., Kuhlmann, H., Holst, C., 2019: Designing and Evaluating a User-Oriented Calibration Field for the Target-Based Self-Calibration of Panoramic Terrestrial Laser Scanners. *Remote Sens*. 12, 15. https://doi.org/10.3390/rs12010015

Nguyen, T.-M., Duberg, D., Jensfelt, P., Yuan, S., Xie, L., 2023: SLICT: Multi-Input Multi-Scale Surfel-Based Lidar-Inertial Continuous-Time Odometry and Mapping. *IEEE Robot. Autom. Lett*. 8, 2102–2109. https://doi.org/10.1109/LRA.2023.3246390

Potokar, E., & Kaess, M., 2025: A Comprehensive Evaluation of LiDAR Odometry Techniques. *arXiv preprint arXiv:2507.16000*.

Shan, T., Englot, B., 2018: LeGO-LOAM: Lightweight and Ground-Optimised Lidar Odometry and Mapping on Variable Terrain, *IEEE/RSJ International Conference on Intelligent Robots and Systems (IROS). IEEE*, pp. 4758–4765. https://doi.org/10.1109/IROS.2018.8594299

Shan, T., Englot, B., Meyers, D., Wang, W., Ratti, C., & Rus, D., 2020: Lio-sam: Tightly-coupled lidar inertial odometry via smoothing and mapping. In *2020 IEEE/RSJ international conference on intelligent robots and systems (IROS)* (pp. 5135-5142). IEEE.

Vizzo, I., Guadagnino, T., Mersch, B., Wiesmann, L., Behley, J., Stachniss, C., 2023: KISS-ICP: In Defense of Point-to-Point ICP – Simple, Accurate, and Robust Registration If Done the Right Way. *IEEE Robot. Autom. Lett*. 8, 1029–1036. https://doi.org/10.1109/LRA.2023.3236571

Wu, Y., Guadagnino, T., Wiesmann, L., Klingbeil, L., Stachniss, C., & Kuhlmann, H., 2024: LIO-EKF: High frequency LiDAR-inertial odometry using extended kalman filters. In *2024 IEEE International Conference on Robotics and Automation (ICRA)* (pp. 13741-13747). IEEE.

Xu, W., Zhang, F., 2021: FAST-LIO: A Fast, Robust LiDAR-Inertial Odometry Package by Tightly-Coupled Iterated Kalman Filter. *IEEE Robot. Autom. Lett*. 6, 3317–3324. https://doi.org/10.1109/LRA.2021.3064227

Yu, W., Xu, J., Zhao, C., Zhao, L., Nguyen, T.-M., Yuan, S., Bai, M., Xie, L., 2024: I 2 EKF-LO: A Dual-Iteration Extended Kalman Filter Based LiDAR Odometry, *IEEE/RSJ International Conference on Intelligent Robots and Systems (IROS)*. IEEE, pp. 10453–10460. https://doi.org/10.1109/IROS58592.2024.10801455

Yuan, C., Xu, W., Liu, X., Hong, X., Zhang, F., 2022: Efficient and Probabilistic Adaptive Voxel Mapping for Accurate Online LiDAR Odometry. *IEEE Robot. Autom. Lett*. 7, 8518–8525. https://doi.org/10.1109/LRA.2022.3187250

Yue, X., Zhang, Y., Chen, J., Chen, J., Zhou, X., & He, M., 2024: LiDAR-based SLAM for robotic mapping: state of the art and new frontiers. *Industrial Robot: the international journal of robotics research and application*, *51*(2), 196-205.

Zhang, J., & Singh, S., 2014: LOAM: Lidar odometry and mapping in real-time. In *Robotics: Science and systems* (Vol. 2, No. 9, pp. 1-9).

Zhang, Z., Scaramuzza, D., 2018: A Tutorial on Quantitative Trajectory Evaluation for Visual(-Inertial) Odometry, *IEEE/RSJ International Conference on Intelligent Robots and Systems (IROS). IEEE*, pp. 7244–7251. https://doi.org/10.1109/IROS.2018.8593941

Zhu, F., Ren, Y., Zhang, F., 2022: Robust Real-time LiDAR-inertial Initialization, *IEEE/RSJ International Conference on Intelligent Robots and Systems (IROS). IEEE*, pp. 3948–3955. https://doi.org/10.1109/IROS47612.2022.9982225